Zagazig University Medical Journal
www.zumj.journals.ekb.eg
https://doi.org/10.21608/zumj.2023.190394.2737 Volume 29, Issue 2, March 2023, Page (728-745)
Manuscript ID ZUMJ-2301-2737
DOI 10.21608/zumj.2023.190394.2737

ORGINAL ARTICLE

Pneumotoxicity of Styrene Oxide and the Possible Protective Role of Thymosin β4 in Albino Rat: Biochemical and Immunohistochemical Study

Ola A. Abdelwahab, Eman R. Abozaid, Reham H. Abdel-Kareem

Corresponding author
*** Ola A. Abdelwahab**
Human Anatomy & Embryology Department, Faculty of Medicine, Zagazig University, Egypt
Email:
olaabdelwahab207@gmail.com
OAMostafa@medicine.zu.edu.eg
Mobile: 01010352110

Submit Date 2023-02-09
Accept Date 2023-02-13

ABSTRACT

Background: Styrene (ST) has been used for plastic and resin production. It was reported to induce injury of pulmonary tissues. Thymosin β4 (Tβ4), a naturally expressed protein, was reported to have antioxidant, anti-inflammatory, antiapoptotic, and regenerative properties. **Aim of study:** This study was designed to examine the role of Tβ4 in ameliorating Styrene Oxide (SO)-induced complication on the lung tissues and its potential mechanisms. **Material and methods:** Forty adult male Wistar albino rats were allocated randomly into 4 groups, 10 rats each. **Control group:** rats were injected intraperitoneally (i.p.) with 0.5cm physiological saline. **Tβ4 group:** rats were injected i.p. with 1mg/kg of Tβ4. **SO group:** rats were injected i.p. with 300 mg/kg of SO. **SO+ Tβ4 group:** rats were concomitantly injected i.p. with 300 mg/kg of SO and 1mg/kg of Tβ4. All chemicals were given once daily for 28 days. **Results:** There was a high significant decrease in the body weight, TAO and GSH levels and a significant increase in lung indices, inflammatory markers (TNF-α, IL-1β, and IL-13) and lipid peroxidation marker (MDA) levels in SO group. Also, there was a high significant increase in TGF-β1 and decrease in PGE2 in the SO group. SO also induced marked histopathological changes in lung tissues involving thickened interalveolar septa, collapsed alveoli, and infiltration by inflammatory cells. Also, there were excess collagen fiber depositions, increased number of macrophage cells, and positive α-SMA, CD68 and VEGF immunoreactivity. These results were significantly ameliorated via Tβ4 administration. **Conclusion:** Tβ4 was effective in preserving the structure and function of the lung after the injury induced by SO.

Keywords: Styrene oxide, Tβ4, BALF, PGE2, TGF-β1

INTRODUCTION

Styrene (ST) is an organic substance that has been used for plastic and resin production since 1940. ST vapor is detected as a contaminant in the air and in the drinking water around manufacturing areas. It is also found in petroleum products produced by the organic molecule-cracking process, polystyrene micro-plastic products, coal tar, gas, and cigarette smoke. International Agency for Research on Cancer (IARC) has considered its metabolite, styrene oxide (SO), as a probably mutagenic substance. SO has a variety of health hazards; being pneumotoxic, hepatotoxic, and neurotoxic [1,2]. Various previous studies have examined these harmful effects using the systemic route of administration [3-6], while others used the route of inhalation [7-9].

Although the mechanism of SO-induced pulmonary injury is not fully known, however, collected data suggests that it may be contributed to oxidative stress and the decrease levels of the non-enzymatic antioxidant as GSH [10,11], caused by this highly reactive metabolite of ST [12].

SO–induced pulmonary injury is proposed to be attributed to the in situ biotransformation of ST or transportation of SO itself to the general circulation from the liver to lung [13].

Thymosin β4 (Tβ4), a G-actin-sequestering protein, is engaged in tissue formation and regeneration [14]. It is expressed in a variety of normal tissues of rat, mouse, and human [15,16].

Additionally, Tβ4 is regarded as a safe compound and a well-tolerated preclinical trial agent in experimental pharmacological and toxicological studies on rats, dogs, monkeys [17], and humans [18].

It was reported that Tβ4 has a systemic antioxidant, anti-inflammatory [19, 20], antiapoptotic and regenerative properties [15]. Also, it was proved to be specifically effective in preventing inflammation and fibrosis of liver [21], and in stimulating healing of eye, skin, and heart [22-24].

In referral to the rising prevalence of mankind use of ST and the potential toxic effects of its metabolite SO on the pulmonary system and the above-mentioned biological efficacy of Tβ4, we have conducted this study to elaborate the probability of Tβ4 to guard against SO-pneumo-toxicity. To the best of our knowledge; this might be a novel experimental research studying possible protective role of Tβ4 against SO-induced pneumotoxicity.

MATERIAL AND METHODS

Chemicals

Styrene oxide (SO) (Sigma-Aldrich, Steinheim, Germany) was dissolved in sterile water with a purity of 97% injected intraperitoneally (i.p.) at a daily dose of 300 mg/kg for 28 days [25]. Thymosin β4 (Tβ4) in a form of Thymosin Beta 500 (TB-500) 10 mg vial (Peptides, SKU: 0013-2) was injected i.p. at a daily dose of 1mg/kg [20] for 28 days.

Animals

Forty adult male Wistar albino rats (12-week-old) weighing 210±15 g were attained from the Scientific and Medical Research Centre's animal house of Faculty of Medicine, Zagazig University (ZSMRC). They were permitted for 1week acclimation preceding the start of research. They were kept in separate cages, fed standard rat pellet chow, and housed in standardized laboratory and ambient conditions. All animal testing was conducted in accordence with the applicable rules and regulations set forth the arrive guidelines [26], followed the international standards for the handling and use of experimental animals [27] and approved by the Institutional Animal Care and Use Committee of Zagazig University (ZU-IACUC committee), approval number ***ZU-IACUC/3/F/303/2022***.

Experiment protocol

The rats were allocated randomly into 4 groups (10 rats each) as follows:

Control group: rats were injected i.p with 0.5cm physiological saline, once daily for 28 days.

Tβ4 group: rats were injected i.p with 1mg/kg of Tβ4 [20], once daily for 28 days.

SO group: rats were injected i.p with 300 mg/kg of SO, once daily for 28 days [25].

SO+ Tβ4 group: rats were concomitantly injected i.p with 300 mg/kg of SO and 1mg/kg of Tβ4, once daily for 28 days.

Preparation of lung tissue samples

24 hours after the last injection, body weight was recorded. Then the rats were anesthetized by i.p. injection of sodium thiopental (100 mg/kg). Half of the rats in each group (5 rats) were utilized for extraction of bronchoalveolar lavage fluid (BALF). The remaining 5 rats were subjected to cervical dislocation, then a midline incision of their chest cavities was done and finally the lungs were dissected and cleaned by ice cold saline. Thereafter, 10% homogenate (W/V) of the left lung was prepared and the supernatant was kept in -80 °C for subsequent biochemical assessment. Then, the right lung tissue was fixed and processed for histological examination as was adopted by Suvarna et al. [28].

Assessment of body weight, lung weight and lung index:

Animals were weighed before being euthanized and each of the removed lungs was weighed. For computing the lung index, the lung weight (g) was divided by body weight (g) then multiplied by 100 [29].

Biochemical measures in the lung tissue homogenate:

Homogenization of lung tissues was done using 1g lung tissue per 10 ml of cold buffer (100 mM potassium phosphate, pH 7.0, containing 2 mM EDTA), then the homogenate was centrifuged for 15 min. at 50,000 rpm. The clear supernatant was collected and kept at –80°C for assessment of the following biochemical parameters:

Assessment of the oxidative stress markers in lung tissue:

Lipid peroxidation was evaluated by assessment of malondialdehyde (MDA) using rat sandwich ELISA kit (MyBioSource, CA, catalog # MBS727531). According to Ellman [30], reduced glutathione (GSH) was measured according to manufacturer's protocol. Total antioxidant capacity (TAO) was evaluated via the manufacturer's colorimetric method (Sigma Co., Cat. NO. MAK187).

Measurement of inflammatory cytokines in lung tissue:

Levels of tumor necrosis factor alpha (TNF-α) and interleukin (IL)-1β were assessed by

ELISA Kits (MyBioSource)_and standard curves were plotted.

Measurement of prostaglandin E2 (PGE2) level in lung tissue:

A competitive enzyme immunoassay kit (Abcam, ab133021, Cambridge, UK) was used to assess the level of PGE in the lung tissue homogenate in accordance with the manufacturer's instructions.

Collection of the broncho-alveolar lavage fluid (BALF):

According to Alsemeh and Abdullah [31], the thoracic cavity was exposed and a 24G cannula was inserted in the trachea. Lavage was done 3 times through this tracheal cannula, where each lung was perfused with 3ml physiologic saline for 30 seconds per lavage. The saline was then aspirated to obtain approximately 9 mL of the BALF (recovery rates of the BALF must be more than 80%).The centrifugation of the collected BALF was done at 2000 rpm for 10 min. at 4 °C, and the supernatant was utilized to measure the level of IL-13 and transforming growth factor β (TGF-β1) in BALF.

Analysis of IL-13 and TGF-β1 in BALF:

IL-13 and TGF-β1 were assessed in BALF by ELISA technique using ELISA kit (R&D System, MN), in accordance with the manufacturer's protocols.

Analysis of lung damage index by measuring total protein levels, lactate dehydrogenase (LDH), and alkaline phosphatase (ALP) activities in BALF:

LDH and ALP were evaluated using LDH activity assay kit (MAK066: Sigma-Aldrich, St Louis, MO, USA) and ALP activity assay kit (291-58601: Wako Chemicals Co., Ltd., Tokyo, Japan), according to the manufacturer's protocols. A protein assay kit was utilized to quantify the total protein content (Bio-Rad, CA) according to the manufacturer's protocols.

Histological examination

Hematoxylin and eosin (H&E) and Masson's trichrome staining:

After fixation of lung tissues in neutral buffered formalin, they were subjected to alcohol dehydration, xylene clearance and then impregnation in paraffin wax forming paraffin blocks. Using a microtome, lung samples were cut into 4–5-micron sections, mounted on glass slides, deparaffinized, and stained with H&E to study the histological changes in the lung architecture and Masson's trichrome staining of collagen fibers for detection of lung fibrosis.

Immunohistochemical examination of alpha smooth muscle actin (α-SMA), cluster of differentiation 68 (CD68) and vascular endothelial growth factor (VEGF) in the lung tissue:

The avidin-biotin-peroxidase technique was utilized.

1. The endogenous peroxidase was blocked by dewaxing paraffin slices of 4-5 µm thickness in xylene, rehydrating in ethanol in decreasing grades, and then embedding them in 0.3% of hydrogen peroxide for 30 minutes.
2. For 15 min, samples were microwaved in citrate buffer (pH: 6) then the antigens were observed.
3. 10 percent goat serum was applied for 30 minutes for inhibiting binding that is not specific.
4. Following a gentle cleaning with PBS, tissue slices were incubated at 4°C overnight with α-SMA antibody from (rabbit monoclonal antibody, 1:500 dilution, Santa Cruz Company, California, USA), with CD68 antibody from (mouse monoclonal antibody, 1:200 dilution, Leica Biosystems, Benton La, Newcastle Ltd, UK) and with VEGF (rabbit monoclonal antibody, 1:500 dilution, Pharminagen, Mississauga, Canada).
5. Finally, counterstaining of slides by Mayer's hematoxylin, dehydration, and fixation by DPX were done. For negative controls, the step of primary antibody addition was replaced by adding PBS. Microscopically, the presence of the immunoreactive cells with a brown color was indicative of positive immunoreactivity for the markers α-SMA, CD68, and VEGF staining.

Morphometric analysis

Image analysis software (ImageJ 1.36b, http://rsbweb.nih.gov/ij) was used for quantitative assessment of the pulmonary tissue by measuring the following parameters in each group: The mean thickness of the lung septum (µm) (in H&E sections), the mean area percent of collagen fibers in Masson's trichrome, and the mean area % of CD68, α-SMA, and VEGF immunoreactivity. All these parameters were assessed in 5 non-overlapped fields for each slide of all studied groups at a magnification of X100. Also, the mean number of lung macrophages situated at the interalveolar septa was counted in immunoreactive CD68 stained sections (at a magnification of X400).

Statistical analysis

A statistical analysis of the biochemical and morphometric results was achieved by GraphPad Prism v. 5 (GraphPad Software, Inc., La Jolla, CA, USA). One-way ANOVA was used for comparing the mean values of the studied groups. Multiple comparisons were assessed by *Tukey's* post-hoc test. P-value less than 0.05 displayed statistical significance, while P-value less than 0.001 displayed high statistical significance.

RESULTS

Effect of styrene oxide (SO) and Tβ4 on the body weight and lung index:

Regarding body weight and lung index, there were high significant decrease in body weight and increase in lung index in the SO group vs control groups (p <0.001), and between SO group vs SO+Tβ4 group. In comparison between controls vs SO+Tβ4 group, there was a highly significant increase in body weight and decrease in lung index (p <0.001) (Fig. 1a, b).

Effect of styrene (SO) and Tβ4 on the oxidative stress markers in the lung tissue:

Regarding the assessed oxidative markers, there were a high significant increase in MDA activities and decrease in TAO and GSH levels in SO group vs control groups (p <0.001), and between SO group vs SO+Tβ4 group. In comparison between control groups vs SO+Tβ4 group, the difference was non-significant in TAO levels with significant decrease in MDA and increase in GSH levels (p < 0.05) (table 1).

Effect of SO and Tβ4 on the inflammatory markers in lung tissue:

Regarding the assessed inflammatory markers, there was a highly significant increase in TNF-α and IL-1β levels in lung tissue and IL-13 in BALF (p<0.001) in the SO group vs control groups and also in SO group vs SO+Tβ4 group. On the other hand, there was a non-significant change in the levels of TNF-α and IL-1β between control group vs SO+Tβ4 group. While there was a significant increase in IL-13 level (p < 0.05) in SO+Tβ4 group vs control groups (table 1)

Effect of SO and Tβ4 on levels of TGF-β1 in BALF and PGE2 in lung tissue:

Regarding markers measured for fibrosis, there were high significant increase in TGF-β1 and decrease in PGE2 in the SO group vs control groups (p<0.001) and also in SO group vs SO+Tβ4 group. In comparison between controls vs SO+Tβ4 group, there were a high significant decrease in TGF-β1 and increase in PGE2 levels (p<0.001) (Fig. 1c, d).

Effect of SO and Tβ4 on total protein levels, (LDH), and (ALP) activities in BALF:

Regarding the indices of lung damage, there were high significant increase in total protein levels, LDH, and ALP activities in the SO group vs control groups (p<0.001) and also in SO group vs SO+Tβ4 group. In comparison between control groups vs SO+Tβ4 group, there were significant decrease in total protein levels (p < 0.05) and high significant decrease in LDH and ALP activities (p<0.001) (table 1).

Effect of SO and Tβ4 on Histological structure of the lung:

1-Histological results of H&E staining:

The lung tissue sections of both control and Tβ4 groups displayed the normal spongy histologic structure. There were thin interalveolar septa separating normal sized alveoli, alveolar sacs, and alveolar ducts. The epithelium of the respiratory bronchioles was intact, and there were healthy blood vessels nearby (Fig.2 a, b).

SO group exhibited disrupting of the histological structure as substantial thickening of the bronchial walls and interalveolar septa, together with multiple collapsed alveoli, which indicated extensive alveolar damage. Also, the lung tissue displayed significant infiltration by inflammatory cells. Additionally, dilated congested thickened blood vessels, and perivascular and peri bronchial infiltrations were seen. There were also areas of interstitial hemorrhage and interstitial exudate (Fig. 2c-e).

In SO+Tβ4 group, restoration of the normal histologic structure was observed except for the presence of thick interalveolar septa and slightly dilated bronchioles and blood vessels (Fig. 2f).

According to morphometric analysis of thickness of interalveolar septa, there was a high significant increase (p<0.001) in SO group vs control group and also between SO group vs SO+Tβ4 group. In comparison between control vs SO+Tβ4 group, the difference was non-significant (Fig. 2g).

2-Histological results of Masson's trichrome staining:

The lung tissues in both control and Tβ4 groups showed normal few collagen fibers deposition (Fig. 3a, b), but collagen fibers deposition was noticeably elevated especially in the surrounding areas of the bronchi and blood vessels and also in the interalveolar gaps in the SO group (Fig. 3c). A little rise in the amount of collagen fibers deposits was seen in SO+Tβ4 group (Fig. 3d).

According to morphometric analysis of the mean area % of collagen fibers, slides from SO group showed high significant elevation (p<0.001) vs control groups. Also, SO+Tβ4 group, there was a highly significant difference (p<0.001) vs both control and SO groups (Fig. 3e).

3-Results of α-SMA immunohistochemical staining:

Both control and Tβ4 groups' lung tissues had few cells with a positive brown cytoplasmic reaction (Fig. 4a, b). However, the SO group lung tissues appeared to be abnormal with excess positive cytoplasmic response in different types of cells especially around the bronchi and around the dilated blood vessels (Fig. 4c, d). On the other hand, the lung tissues of the SO+Tβ4 group had few cells with brown positive cytoplasmic reactions (Fig. 4e).

According to morphometric analysis of mean area % of positive α-SMA immuno-stained cells, there was a highly significant increase ($p<0.001$) in SO group vs control groups. Also, there was a high significant difference ($p<0.001$) between SO+Tβ4 group vs both control and SO groups (Fig. 4f).

4-Results of CD68 immunohistochemical staining:

Both control and Tβ4 groups' lung tissues exhibited very few cells with positive cytoplasmic reactions of CD68 (Fig. 5a, b). However, the lungs of the SO group displayed an excess number of macrophage cells with an apparent positive cytoplasmic reaction (Fig. 5c). On the other hand, the lungs of the SO+Tβ4 group had few cells with positive brown cytoplasmic reaction (Fig. 5d).

As regard morphometric analysis of the mean area % of positive CD-68 and the mean macrophage cell count, there was a high significant increase ($p<0.001$) in SO group when compared to control group. Also, there was a high significant difference ($p<0.001$) between SO+Tβ4 group vs both control and SO groups (Fig. 5e, f).

5-Results of VEGF immunohistochemical staining:

A very little positive brown cytoplasmic reaction was noticed in the lung tissue of both control and Tβ4 groups (Fig. 6a, b). However, SO group showed various cells with abundant positive cytoplasmic reactions (Fig. 6c). Conversely, SO+Tβ4 group displayed only a small number of cells with brown cytoplasmic reaction (Fig. 6d).

As regard morphometric analysis of the mean area % of positive VEGF stained brown cells, there was a highly significant increase ($p<0.001$) in SO group when compared to control groups. Also, there was a highly significant difference ($p<0.001$) between SO+Tβ4 group vs SO group while the difference was significant ($p<0.05$) between SO+Tβ4 group vs control group (Fig. 6e).

Table (1): Showing the $\overline{X} \pm SD$ of oxidative stress markers, inflammatory markers and indices of lung damage in the different studied groups. Significant difference is considered when $P<0.05$. a: SO group vs Control groups, b: SO group vs SO+Tβ4, and c: Control groups vs SO+Tβ4. Duplication of the symbols (**aa, bb, cc**) means that the difference is highly significant ($P<0.001$).

Groups / Parameters		Control	Tβ4	SO	SO+ Tβ4
MDA (nmol/mg protein)	$\overline{X} \pm SD$	8.4 ±3.13	9.02± 2.02	40.65± 4.63 aa	14.11± 3.13 bb c
TAO (mg/gm protein)	$\overline{X} \pm SD$	30.76± 3.25	33.11± 2.95	21.68 ±4.95 aa	29.71± 2.45 bb
GSH (nmol/mg protein)	$\overline{X} \pm SD$	35.96± 1.39	36.42± 1.28	19.11± 1.17 aa	34.02± 1.83 bb c
TNF-α (pg/mg protein)	$\overline{X} \pm SD$	30.18 ±1.49	28.76 ±1.14	94.09 ±4.56 aa	33.26 ±2.51 bb
IL-1 β (pg/ mg protein)	$\overline{X} \pm SD$	9.98±1.49	8.56±1.14	75.32±4.90 aa	13.19±2.40 bb
IL-13 (pg/ml) BALF	$\overline{X} \pm SD$	0.51 ±0.03	0.536 ±0.03	13.62 ±1.92 aa	6.75 ±1.03 bb c
Total protein (μg/ml) BALF	$\overline{X} \pm SD$	132.5 ± 12.28	131.33 ± 13.87	207.9 ± 8.25 aa	118.6 ± 5.03 bb c
LDH activity (mU/ml) BALF	$\overline{X} \pm SD$	0.71 ± 0.06	0.7 ± 0.06	4.95 ± 0.5 aa	3.22 ± 0.39 bb cc
ALP activity (U/L) BALF	$\overline{X} \pm SD$	990.7 ± 157.11	1057.5±152.26	4226.2±510.1 aa	2552.1 ± 156.96 bb cc

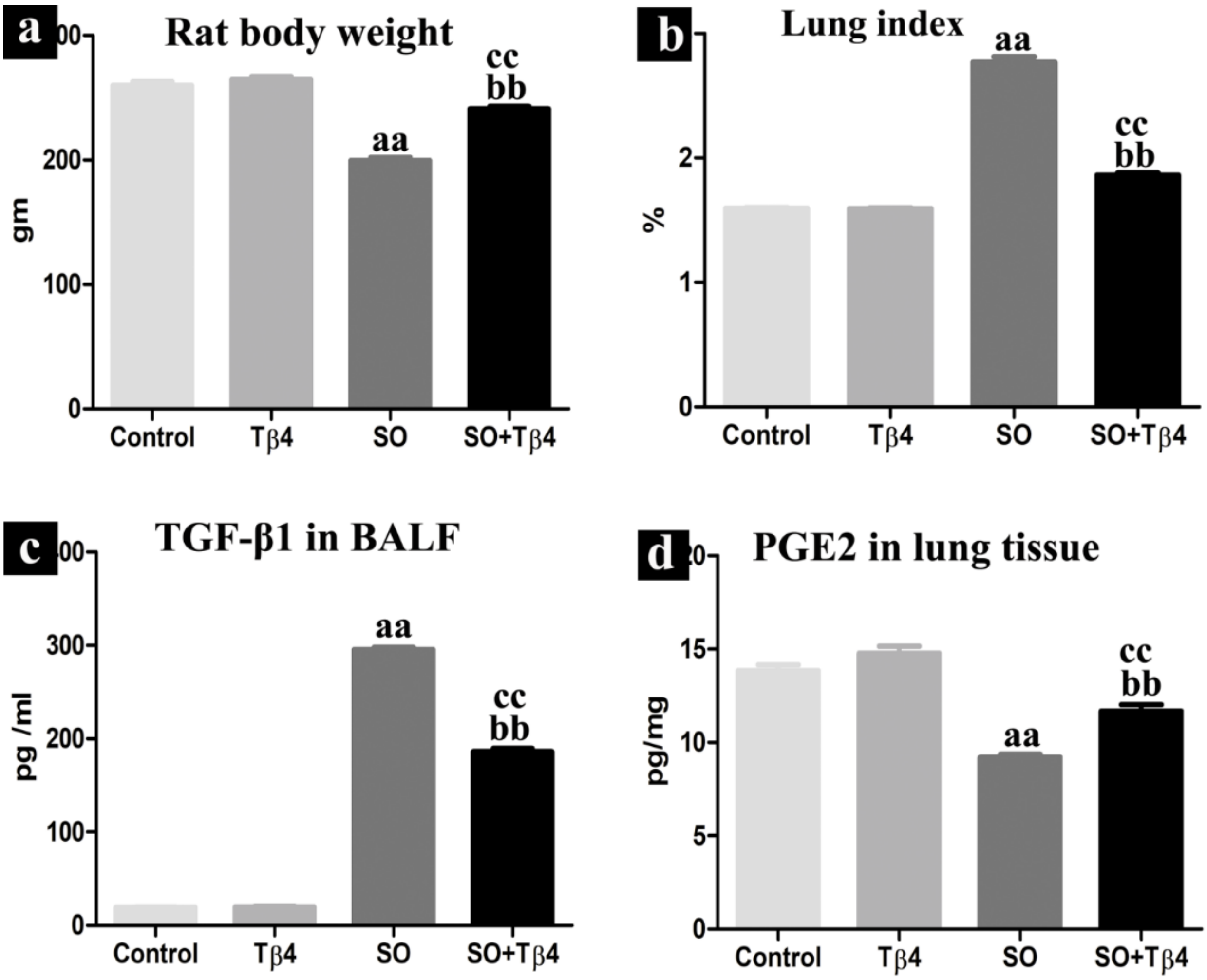

Figure (1): (a,b) bar charts showing morphometrical analysis for body weight and lung index in the different studied groups. (c,d) bar charts showing morphometrical analysis for levels of TGF-β in BALF and PGE2 in lung tissue in different studied groups. Significant difference is considered when $P<0.05$. a: SO group vs Control group, b: SO group vs SO+Tβ4, and c: Control group vs SO+Tβ4. Duplication of the symbols (**aa, bb, cc**) means that the difference is highly significant ($P<0.001$).

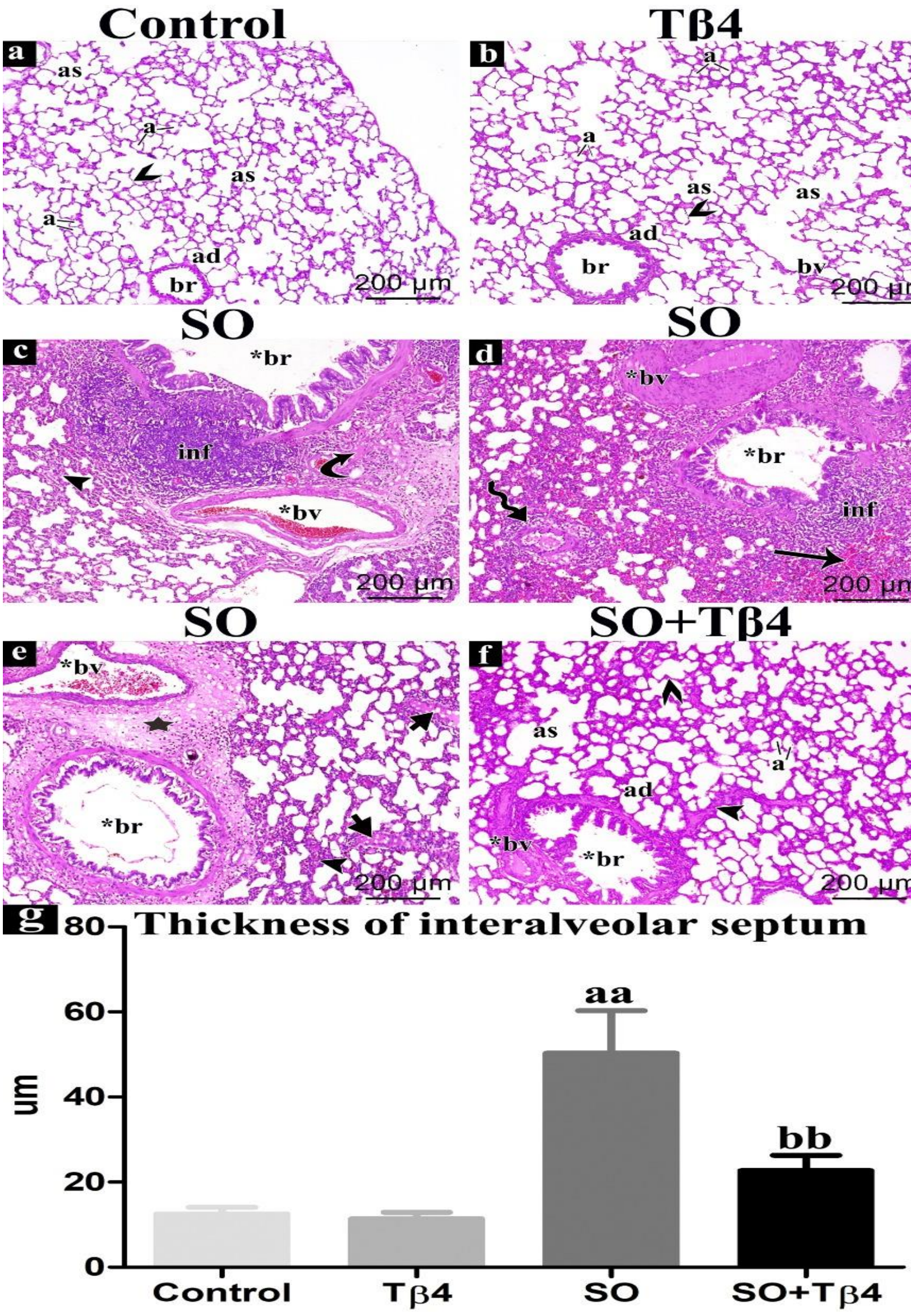

Fig. (2):

Figure (2): photomicrographs of H&E-stained sections of the lung tissue from all groups. In both control (a) and Tβ4 groups (b), lung tissue appears normal with normal alveolar ducts (ad), alveolar sacs (as), and alveoli (a) separated by thin interalveolar septa (empty arrowhead) along with normal respiratory bronchiole (br) and normal blood vessel (bv). In SO group (c, d, e), lung tissue demonstrates areas with thick interalveolar septa (arrow head), peri bronchial (inf) and perivascular (wavy arrow) inflammatory cellular infiltration. Interstitial exudate (short arrow), perivascular exudate (curved arrow), interstitial hemorrhage (thin arrow), and dilated congested fbrosed blood vessel (*bv) appear also. Notice also dilated distorted bronchiole (*br) and collapsed consolidated alveoli (Star). In SO+Tβ4 group (f), slight restoration of the normal histology of the lung tissue appears. Alveolar sacs (as), alveolar ducts (ad) and alveoli (a) are slightly normal. There are areas of thin (empty arrowhead) and thick (arrow head) interalveolar septa. The bronchiole (*br) and the blood vessel (*bv) are slightly dilated. (g) Bar chart showing morphometrical analysis for the thickness of interalveolar septa in the different studied groups. The difference is significant when (P<0.05) as follows, **a:** SO group vs Control group, **b:** SO group vs SO+Tβ4, and **c:** Control group vs SO+Tβ4. Duplication of the symbols (**aa, bb, cc**) means that the difference is highly significant (P<0.001).

Fig. (3):

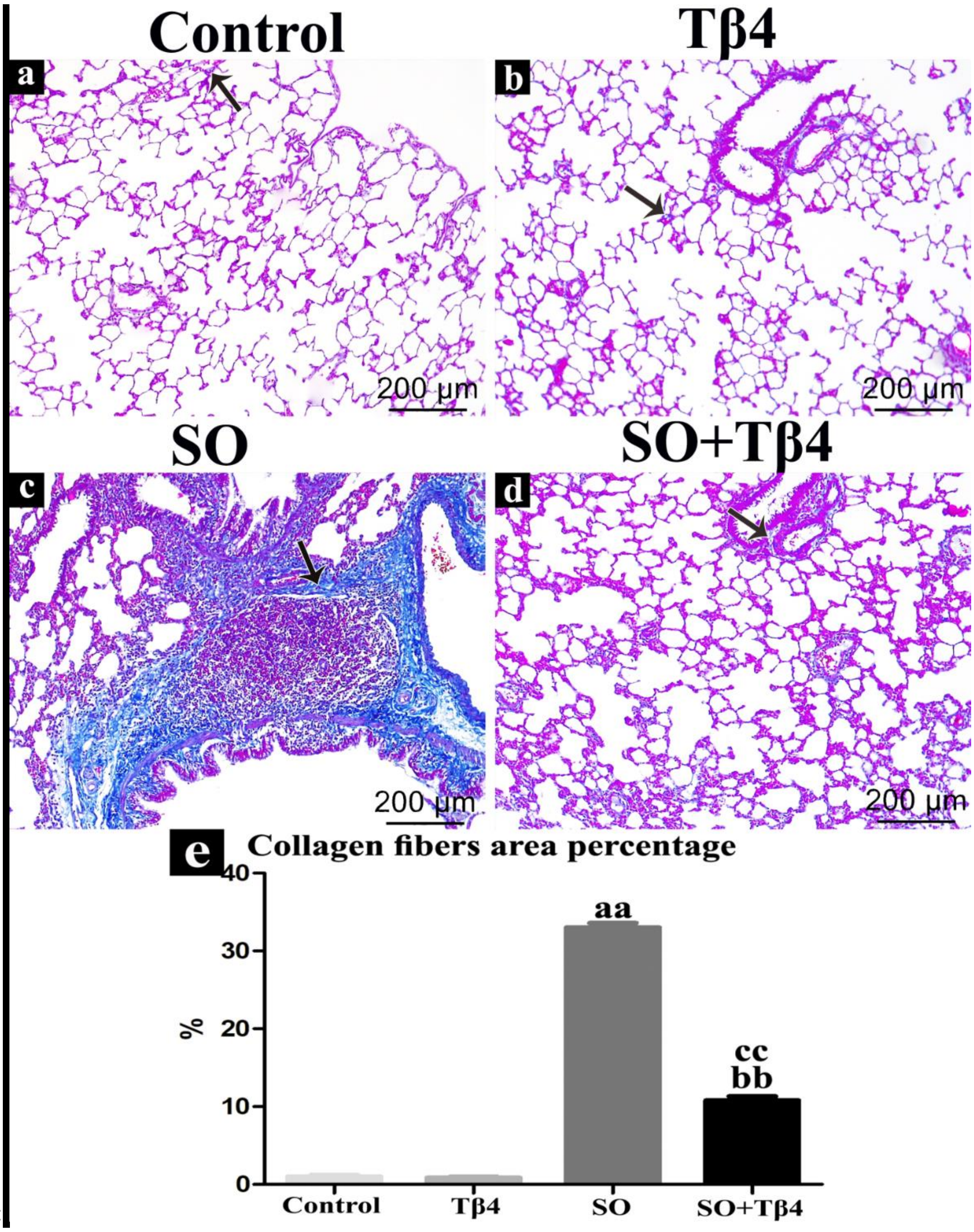

Figure (3): photomicrographs of Masson's trichrome stained sections of the lung tissue from all groups demonstrating collagen fibers in blue color (thin arrow). In both control (a) and Tβ4 groups (b), there are few collagen fibers but in SO group (c), there are excess amounts of collagen fibers. In SO+Tβ4 group, the fibers amount is moderate. (e) Bar chart showing morphometrical analysis for the area percentage of collagen fibers in the different studied groups. The difference is significant when ($P<0.05$) as follows, **a:** SO group vs Control group, **b:** SO group vs SO+Tβ4, and **c:** Control group vs SO+Tβ4. Duplication of the symbols (**aa, bb, cc**) means that the difference is highly significant ($P<0.001$).

https://doi.org/10.21608/zumj.2023.190394.2737 Volume 29, Issue 2, March 2023, Page (728-745)

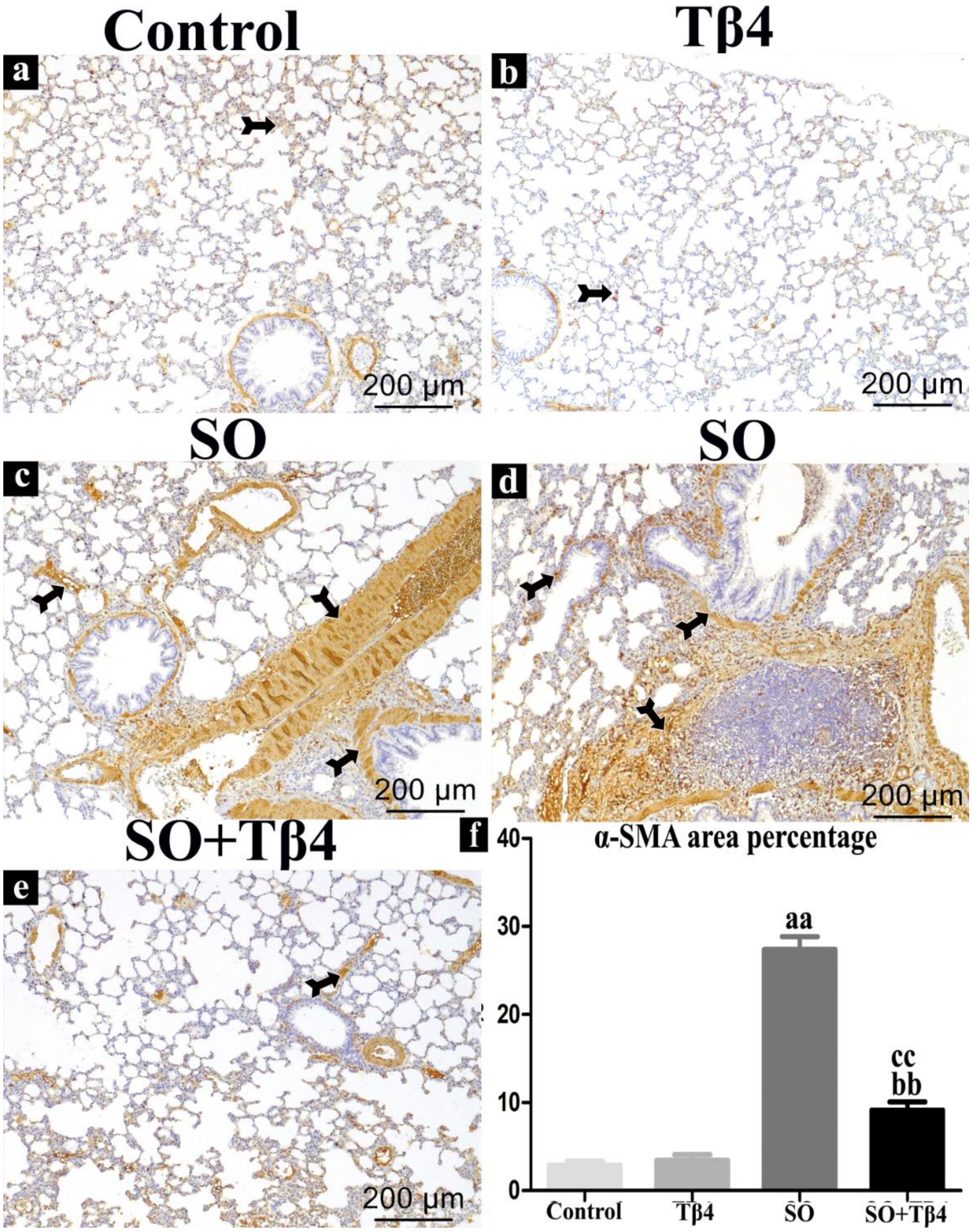

Fig. (4):

Figure (4): photomicrographs of alpha smooth muscle actin (α-SMA) immuno-stained lung tissue sections from all groups showing the degree of immunoexpression. Positive cells with a brown reaction are referred to as (Thick crossed arrow). Control group (a), Tβ4 group (b), SO group (c, d), and SO+Tβ4 group (e). (f) Bar chart showing morphometrical analysis for the area percentage of (α-SMA) immunoreactivity in the different studied groups. The difference is significant when ($P<0.05$) as follows, **a:** SO group vs Control group, **b:** SO group vs SO+Tβ4, and **c:** Control group vs SO+Tβ4. Duplication of the symbols (**aa, bb, cc**) means that the difference is highly significant ($P<0.001$).

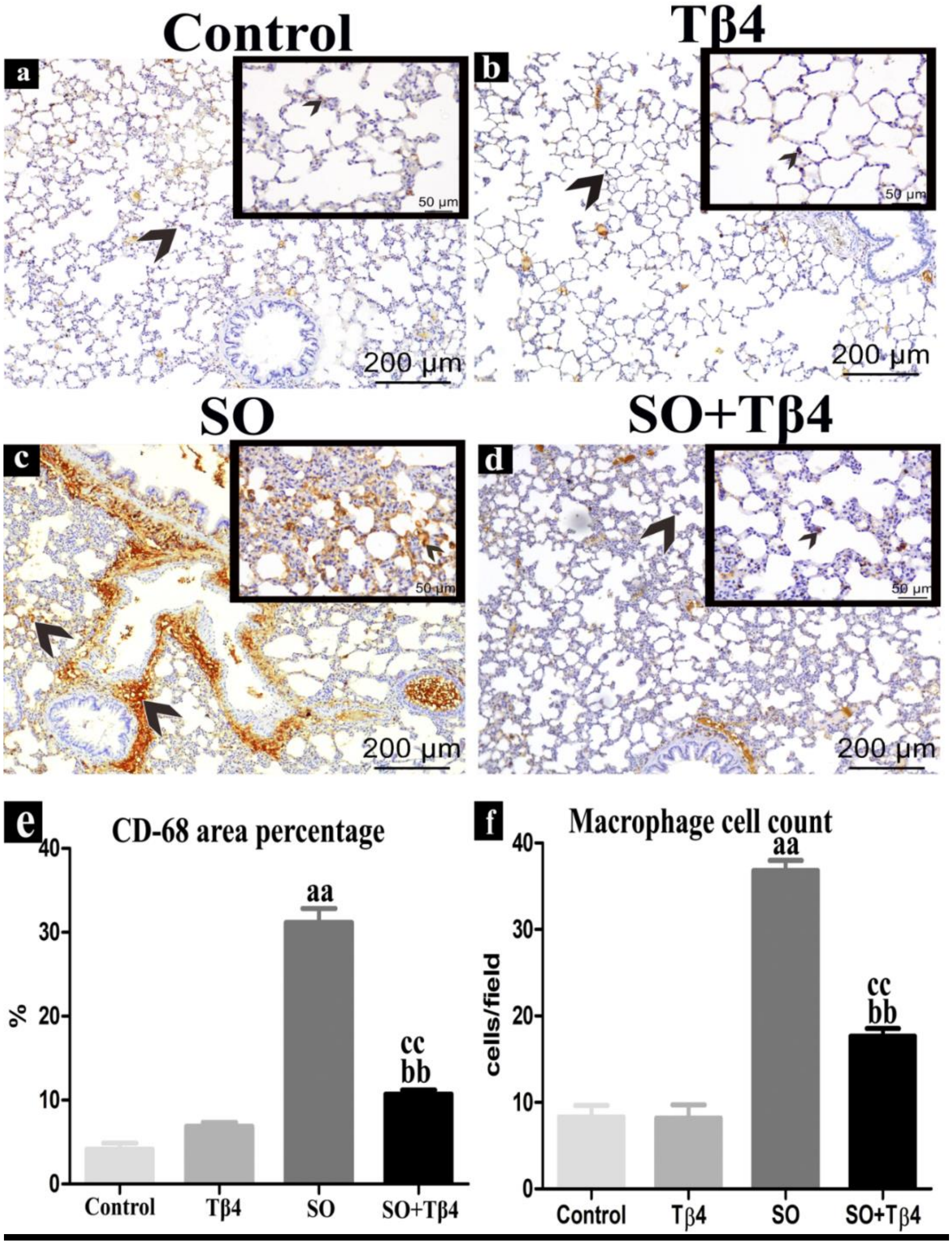

Fig. (5):

Figure (5): photomicrographs of (CD-68) immuno-stained lung tissue sections from all groups showing the degree of immunoexpression. Positive cells with a brown reaction are referred to as (empty arrow head). Control group (a), Tβ4 group (b), SO group (c), and SO+Tβ4 group (d). (e, f) Bar chart showing morphometrical analysis for the area percentage of (CD-68) immunoreactivity and macrophage cell count respectively in the different studied groups. The difference is significant when (P<0.05) as follows, **a:** SO group vs Control group, **b:** SO group vs SO+Tβ4, and **c:** Control group vs SO+Tβ4. Duplication of the symbols (**aa, bb, cc**) means that the difference is highly significant (P<0.001).

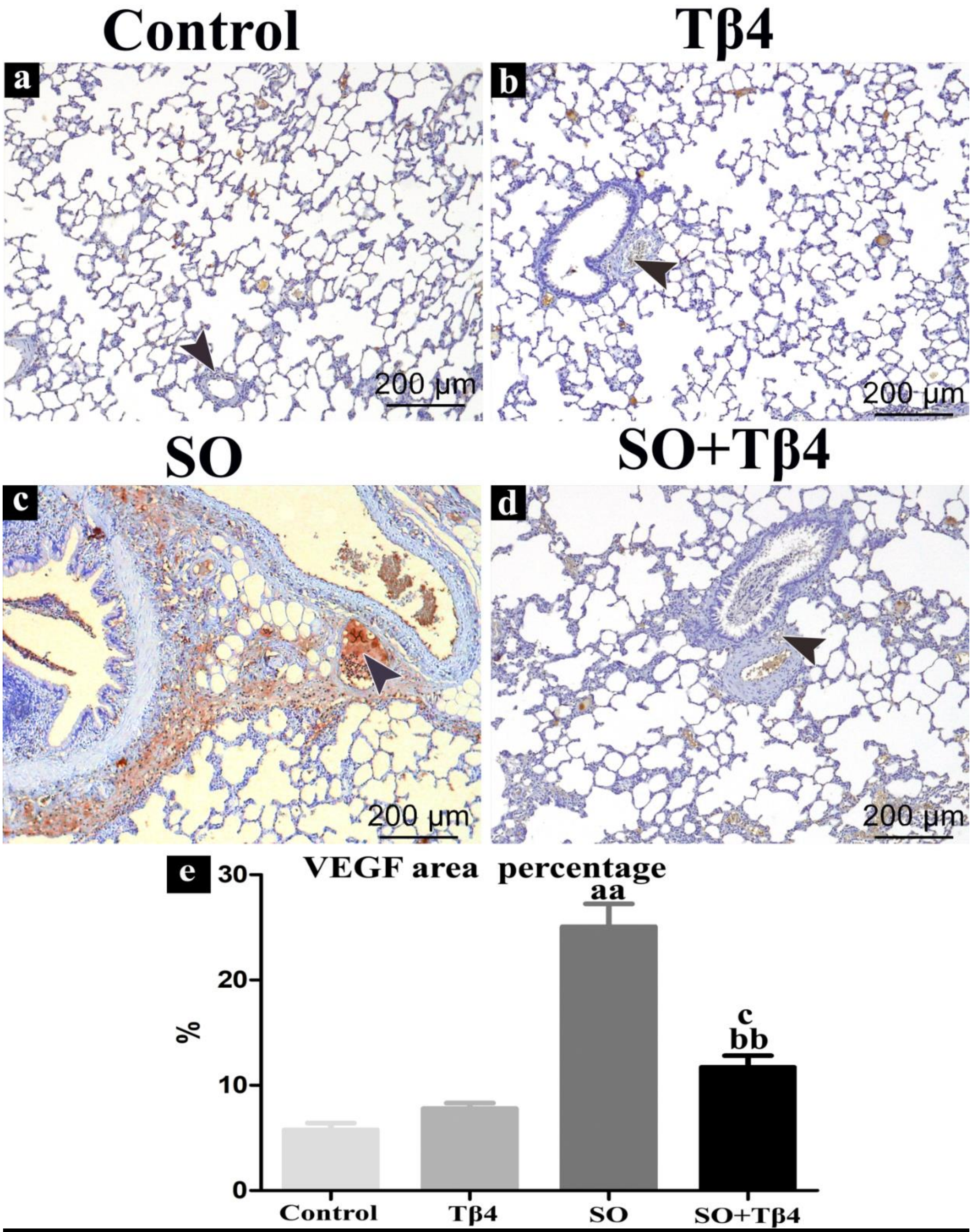

Fig. (6):

Figure (6): photomicrographs of vascular endothelial growth factor (VEGF) immuno-stained lung tissue sections from all groups showing the degree of immunoexpression. Positive cells with a brown reaction are referred to as (arrow head). Control group (a), Tβ4 group (b), SO group (c), and SO+Tβ4 group (d). (e) Bar chart showing morphometrical analysis for the area percentage of (VEGF) immunoreactivity in the different studied groups. The difference is significant when (P<0.05) as follows, **a:** SO group vs Control group, **b:** SO group vs SO+Tβ4, and **c:** Control group vs SO+Tβ4. Duplication of the symbols (**aa, bb, cc**) means that the difference is highly significant (P<0.001).

DISCUSSION

In this study, the pneumotoxic effects of SO were studied using the ip route rather than the inhalation route to assure the dose of exposure to the metabolite and control its level. This systemic route of administration was performed also by various studies that examined these harmful effects [3-6]. Moreover, the pneumotoxicity of systemic styrene tended to be more severe than those reported in the animals exposed to styrene via inhalation for longer periods of time [3].

According to the collected data, the rats' final body weights significantly decreased in the SO group while their lung indices significantly increased, mainly due to SO-induced pulmonary fibrosis, increased deposition of inflammatory cells specially macrophages, and increased thickness within the interalveolar septa. In contrary, Arab **et al.** [7] revealed no significant changes in the body and lung weights after ST exposure. This may be attributed to the shorter period of exposure (18 days) and the different route of administration (inhalation). In the current study, Tβ4 administration with SO improved statistically the rats' body weight and their lung indices which reflected the histological alteration toward normalization in the SO+Tβ4 group.

In the current study, a considerable increase in the levels of TNF-α, IL-1β, and IL-13 in lung tissues was noticed in SO group. These proinflammatory cytokines noted throughout the inflammatory reaction according to Chitra et al. [32], were directly related to the excessive deposition of alveolar macrophages, proved by CD68, as the macrophages represent a predominant producer of these cytokines in referral to Zhang and An [33]. According to Padgett et al. [34], the proinflammatory cytokines are induced by reactive oxygen species (ROS), furthermore, Forrester et al. [35] reported that these cytokines use ROS as part of their signaling cascades, which means increased activity of ROS in concordance to increased levels of the proinflammatory cytokines. These findings were consistent with Kik et al. [36] who referred to the increased activity of ROS in relation to ST exposure.

While, in SO+Tβ4 group, there was a significant decrease in TNF-α, IL-1β, and IL-13 levels due to the decreased deposition of alveolar macrophages observed by CD68. This confirms the anti-inflammatory impact of Tβ4. Such results were recorded also in previous researches, where systemic Tβ4 injection lowered the TNF-α level in mice with sepsis, intestinal I/R injury, and experimental colitis [37-39]

Oxidative stress is a major factor in lung fibrosis [40]. The etiology of fibrosis involves the production of ROS [41,42]. Additionally, pulmonary fibrosis in patients as well as animal models was shown to contain signs of oxidative stress [32].

There was serious affection of the oxidant-antioxidant balance in the SO group. In this study SO group exhibited markedly increased MDA level along with decreased GSH and TAO activities in lung tissues. This was in concordance with Haghighat et al. [43] who exposed the rat's lung to 750 ppm of ST for 4 weeks and recorded an elevation of MDA level and reduction of catalase, superoxide dismutase, and GSH activities.

Dramatically, Tβ4 therapy in SO+Tβ4 group decreased MDA and elevated TAO and GSH levels in the lung tissue, proving its effectiveness as an antioxidant and ROS scavenger in the lung. Furthermore, Tβ4 anti-inflammatory properties may be also responsible for its anti-oxidative action in lung tissue. Consistent with earlier research, Tβ4 therapy was shown to lower ROS levels by boosting Superoxide dismutase (SOD) activity in corneal and cardiac damage [44]. It also promotes autophagy, epithelial barrier defense, and repair owing to its antioxidant and antiapoptotic properties [44,45].

Interestingly, our results showed a dramatic rise of TGF-β1 in BALF of SO group. TGF-β1 is the most potent cytokine known to promote fibrosis according to Wei et al. [44] and Renga et al. [45]. This rise of TGF-β1 is in harmony with the histological findings of pulmonary fibrosis and the data interpreted from Masson's trichrome and α-SMA and that proved to be statistically significant.

According to Horowitz et al. [46] and Tseng et al. [47], TGF-β1 can promote pulmonary fibroblasts' production of collagen and/or cause fibroblasts to change into myofibroblasts that produce α-SMA, both of which are essential for development of lung fibrosis.

Independently of TGF- β1, another profibrotic cytokine, IL-13, a T-helper type 2 cytokine, can promote fibroblast collagen synthesis [48]. TGF-β1 levels together with the levels of the above measured pro-inflammatory cytokines were critically responsible for fibroblast development.

However, a considerable decline in the BALF level of TGF-β1 and the pro-inflammatory cytokines was observed in SO+Tβ4 group, suggesting that Tβ4 has antifibrotic properties.

Even, in malignant gliomas, Tβ4 modifies key molecular networks such as p53 and TGF-β1 signaling. [49]. However, Smart et al. [50] showed no appreciable alterations in the expression of a variety of TGF-β1 by Tβ4 in the adult epicardium. We suggest that the modulation of TGF-β1 levels induced by Tβ4 varies according to the cells' behaviors during different diseases.

Interesting evidence suggests that PGE2 may restrict fibrotic responses in the lung. Earlier studies on patients with idiopathic pulmonary fibrosis showed significantly reduced cyclooxygenase-2 (COX-2) expression, which in turn resulted in decreased PGE2 generation in broncho-alveolar fluid and fibroblasts [51,52]. Maher et al. [53] proposed that in the fibrotic lung, the decreased COX-2 and PGE2 levels encourage fibroblast longevity and inhibit its death. And even more, PGE2 can reduce the ability of lung fibroblasts to proliferate, activate, and produce collagen [54].This was in harmony with the findings of the present study, as PGE2 was found to be considerably lower in the SO group, which showed the marked fibrotic changes in the lung, while it proved to be significantly higher in the lung tissue of the SO+Tβ4 group with the minimal fibrotic changes. On the contrary, Hwang et al. [55] reported that β-thymosin suppressed Nitric oxide and PGE_2 production and inflammatory cytokines expression in macrophage cells.

The histopathological findings of the current study mirrored the biochemical results of the different groups. H&E stained sections of SO group showed; multiple collapsed alveoli, infiltration by inflammatory cells, dilated congested blood vessels, interstitial hemorrhage, and edema, this was consistent with the study of Arab et al. [7]. The lung tissue injuries may be due to low lung levels of the main antioxidant GSH [4] that also increased the risk of tumor development in experimental animals [56], and caused cell damage and lysis in different organs [25].

The thicknesses of the interalveolar septa showed significant increase in SO group in comparison with control groups**,** this was supported by the results of Coccini et al**.** [3]**,** Arab et al. [7] and Haghighat et al. [57]. The increased thickness of the interalveolar septa may be explained by the histological findings of increased cellular proliferation in lung alveoli, in agreement with Kaufman et al. [58], capillary dilation, and interalveolar infiltration, in concordance with Yaman et al. [59].

On the other hand, in SO+Tβ4 group, Tβ4 established a histological improvement in response to SO-induced pneumotoxicity. This may be attributed to the measured antioxidant impact of Tβ4, which–raises the expression of antioxidant enzymes and enhances mitochondrial membrane potential against oxidative stress [19]. In support of our findings, Yaman et al. [59] prove**d** the ability of Tβ4 to protect against acute lung injury brought on by ischemia-reperfusion (IR). Prior to ischemia or after reperfusion, Tβ4 treatment resulted in a considerable improvement in the histology of the lung tissue, interalveolar septa's thickness had lessened noticeably, and the recovery of the morphologic changes and damage brought on by IR.

This was parallel with the findings of Gilbane et al. [60] and Kendall and Feghali-Bostwick [61] who also added that myofibroblasts embrace a characteristic population of mesenchymal cells over expressing α-SMA and excessively accumulate fibrillar collagens.

In our study SO-induced pulmonary fibrosis was indicated histologically by presence of fibrotic areas in Masson's trichrome stained sections and also by increased expression of α-SMA immunostaining. These results were in agreement with Li et al. [9] who revealed that inhalation of the polystyrene microplastics in mice for three weeks induced pulmonary fibrosis in a dose-depending manner and stated that the damaged epithelial cells encouraged α-SMA and collagen expression in fibroblasts of lung.

On the contrary, the study done by Lim et al. [8] to identify the effect of inhalation of polystyrene microplastics on lung fibrosis in rats, detected no significant histopathological changes for the Masson's trichrome staining. This was justified to be as a result of the different exposure routes, as systemic exposure has a higher absorption rate than inhalation exposure [62]. Moreover, only some microplastics can enter the lower airways because they are mostly removed from the lungs by the mucociliary clearance [62,63]. While, in agreement with our study Lim et al. [8] evaluated the expression of the markers related to lung fibrosis, and detected a propensity for elevated expression of TGF-β1and TNF- α in a dose-depending manner.

Tβ4 also proved statistically to reduce the area percent of α-SMA-immunoreactivty in the SO+Tβ4 group, along with the decrease in fibrotic areas in Masson stain in the lung tissue. This is in concordance with the decrease in TGF-β1 levels detected in broncho-alveolar fluid in these rats. In the same line, Shah et al. [20] detected Tβ4 suppression of the protein expression of α-SMA and platelet-derived growth factor-β receptor, thereby preventing the differentiation of the myofibroblasts and thus preventing liver fibrosis encouraged by chronic ethanol and acute lipopolysaccharide exposure .

CD68 is an essential membrane glycoprotein expressed by tissue macrophages [64]. The expression of the pan-macrophage marker CD68 is correlated with macrophages' phagocytic activity [65]. In the current study, CD68 immunoreactivity showed significant rise in the percent of positive area stained with CD68 and also the alveolar macrophage cell count in SO group in comparison to control groups. This may be enlightened by lung injury and fibrosis triggered by SO, which sequentially activates lung macrophages and other inflammatory cells.

According to Daghigh et al. [66], the macrophages can produce a chemotactic material that attracts neutrophils and causes them to release proteases and destructive oxygen free radicals that induce tissue damage. However, CD68 immunoreactivity showed significant decrease in the percent of positive area stained with CD68 and also the alveolar macrophage cell count in SO+Tβ4 group, this is in line with the decrease of inflammatory and oxidative markers in lung tissues caused by Tβ4.

VEGF is a cytokine that promotes angiogenesis both during the formation of tumors and in developing embryos [67]. Fibrosis, fibrin turnover, fluid loculation, and inflammation are all regulated by VEGF [68]. This explained the collected data of elevated VEGF immunoreactivity in the SO group, proving the contribution in ST inducd lung tissue injury and fibrosis.

Interestingly, VEGF immunoreactivity showed significant decrease in SO+Tβ4 group, this is in line with the biochemical and histological improvements in this group.

Additionally, in the fibrotic areas of Bleomycin-induced pulmonary fibrosis, Fehrenbach et al. [67] showed a significant increase in VEGF-A positive stained cells in the absence of enhanced vascularization, suggesting that VEGF may affect more than only the vasculature; it may also contribute to the onset of pulmonary fibrosis.

Previously Tβ4 has demonstrated therapeutic effectiveness in inhibiting fibrosis. This was related to a reduction in the inflammatory response, which included a reduction in macrophage infiltration, levels of TGF-β1 and IL-10, and a reduction in the activation of connective tissue growth factors. This prevented fibroblasts from converting into myofibroblasts and also the production of collagen fibers with a normal alignment [70].

CONCLUSION

Both the biochemical and histopathological findings in addition to the morphometric analysis confirm the harmful effect of styrene oxide (SO) on lung tissue and spotlight the probable protecting role of Tβ4 against styrene-promoted lung damage through its anti-inflammatory and regenerative properties. Also, Tβ4 caused improvement in CD68 which reflect the macrophage activity and in turn contributes to its anti-inflammatory and antioxidant, and antiapoptotic effects

In addition, Tβ4 restored TGF-β1 and PGE2 to the normal levels, also α-SMA and VEGF immunoreactivity which could be new antifibrotic and protective mechanisms for Tβ4 in this model. To the greatest of our knowledge, it is the first research to observe the possible relation between Tβ4 and PGE2 and also VEGF in fibrosis prevention. Whether these roles are due to interaction between these pathways or just a coincidence necessitates further proofs. These results imply that Tβ4 has the potential to be fully effective against a variety of fibrosis-related human illnesses. Unresolved issues call for additional research.

REFERENCES

1. Nett RJ, Cox-Ganser JM, Hubbs AF, Ruder AM, Cummings KJ, Huang Y-CT, et al. Non-malignant respiratory disease among workers in industries using styrene—A review of the evidence. Am. J. Ind. Med. 2017; 60:163-180. doi: https://doi.org/10.1002/ajim.22655.
2. Bansal A and Simon MC. Glutathione metabolism in cancer progression and treatment resistance. J Cell Biol. 2018; 217:2291-2298. doi: 10.1083/jcb.201804161.
3. Coccini T, Fenoglio C, Nano R, Polver PDP, Moscato G and Manzo L. STYRENE-INDUCED ALTERATIONS IN THE RESPIRATORY TRACT OF RATS TREATED BY INHALATION OR INTRAPERITONEALLY. *J Toxicol Environ Health* 1997; 52:63-77. doi: 10.1080/00984109708984053.
4. Carlson GP. Depletion by Styrene of Glutathione in Plasma and Bronchioalveolar Lavage Fluid of Non-Swiss Albino (NSA) Mice. *J. Toxicol. Environ. Health Part A* 2010; 73:766-772. doi: 10.1080/15287391003689143.
5. Carlson GP, Turner M and Mantick NA. Effects of styrene and styrene oxide on glutathione-related antioxidant enzymes. J Toxicol 2006; 227:217-226. doi: https://doi.org/10.1016/j.tox.2006.08.006.
6. Ahmadizadeh M, Pol T and Boazar M. Effect of Vitamin C on Styrene Induced Respiratory Toxicity. *Int J Occup Hyg* 2011; 3:76-80.
7. Arab MR, Mirzaei R and Aval FS. The Protective Effects of Gadolinum Chloride on Pneumotoxic Effects of Styrene in Rat. Cell J 2015; 17:422-8. doi: 10.22074/cellj.2015.3.
8. Lim D, Jeong J, Song KS, Sung JH, Oh SM and Choi J. Inhalation toxicity of polystyrene micro(nano)plastics using modified OECD TG 412. Chemosphere 2021; 262:128330. doi: https://doi.org/10.1016/j.chemosphere.2020.128330.
9. Li X, Zhang T, Lv W, Wang H, Chen H, Xu Q, et al. Intratracheal administration of polystyrene microplastics induces pulmonary fibrosis by activating oxidative stress and Wnt/β-catenin signaling pathway in mice. Ecotoxicol Environ Saf 2022; 232:113238. doi: https://doi.org/10.1016/j.ecoenv.2022.113238.
10. Mögel I, Baumann S, Böhme A, Kohajda T, von Bergen M, Simon J-C, et al. The aromatic volatile

organic compounds toluene, benzene and styrene induce COX-2 and prostaglandins in human lung epithelial cells via oxidative stress and p38 MAPK activation. J Toxicol 2011; 289:28-37. doi: https://doi.org/10.1016/j.tox.2011.07.006.

11. Sati PC, Khaliq F, Vaney N, Ahmed T, Tripathi AK and Banerjee BD. Pulmonary function and oxidative stress in workers exposed to styrene in plastic factory: Occupational hazards in Styrene-exposed plastic factory workers. Hum Exp Toxicol 2011; 30:1743-1750. doi: 10.1177/0960327111401436.
12. Boogaard PJ, de Kloe KP, Wong BA, Sumner SCJ, Watson WP and van Sittert NJ. Quantification of DNA Adducts Formed in Liver, Lungs, and Isolated Lung Cells of Rats and Mice Exposed to 14C-Styrene by Nose-Only Inhalation. Toxicol Sci 2000; 57:203-216. doi: 10.1093/toxsci/57.2.203.
13. Massumeh A, Tayebeh P and Mohammad B. Effect of Vitamin C on Styrene Induced Respiratory Toxicity. J Occup. Hyg. 1970; 3.
14. Bollini S, Riley PR and Smart N. Thymosin β4: multiple functions in protection, repair and regeneration of the mammalian heart. Expert Opin Biol Ther 2015; 15:163-174. doi: 10.1517/14712598.2015.1022526.
15. Crockford D, Turjman N, Allan C and Angel J. Thymosin β4: structure, function, and biological properties supporting current and future clinical applications. Ann N Y Acad Sci 2010; 1194:179-189. doi: https://doi.org/10.1111/j.17496632.2010.05492.x.
16. Jo J-O, Kang Y-J, Ock MS, Kleinman HK, Chang H-K and Cha H-J. Thymosin β4 Expression in Human Tissues and in Tumors Using Tissue Microarrays. Appl Immunohistochem Mol Morphol 2011; 19:160-167. doi: 10.1097/PAI.0b013e3181f12237
17. Philp D and Kleinman HK. Animal studies with thymosin β4, a multifunctional tissue repair and regeneration peptide. Ann N Y Acad Sci 2010; 1194:81-86. doi: https://doi.org/10.1111/j.1749-6632.2010.05479.x.
18. Zhu J, Song J, Yu L, Zheng H, Zhou B, Weng S, et al. Safety and efficacy of autologous thymosin β4 pre-treated endothelial progenitor cell transplantation in patients with acute ST segment elevation myocardial infarction: A pilot study. Cytotherapy 2016; 18:1037-1042. doi: https://doi.org/10.1016/j.jcyt.2016.05.006.
19. Ho JH-C, Tseng K-C, Ma W-H, Chen K-H, Lee OK-S and Su Y. Thymosin beta-4 upregulates anti-oxidative enzymes and protects human cornea epithelial cells against oxidative damage. *Br J Ophthalmol* 2008; 92:992-997. doi:10.1136/bjo.2007.136747.
20. Shah R, Reyes-Gordillo K, Cheng Y, Varatharajalu R, Ibrahim J and Lakshman MR. Thymosin <i>β</i>4 Prevents Oxidative Stress, Inflammation, and Fibrosis in Ethanol- and LPS-Induced Liver Injury in Mice. *Oxid Med Cell Longev*; 2018:9630175. doi: 10.1155/2018/9630175.
21. Kim J, Wang S, Hyun J, Choi SS, Cha H, Ock M, et al. Hepatic stellate cells express thymosin Beta 4 in chronically damaged liver. PloS one 2015; 10:e0122758.
22. Bock-Marquette I, Saxena A, White MD, Michael DiMaio J and Srivastava D. Thymosin β4 activates integrin-linked kinase and promotes cardiac cell migration, survival and cardiac repair. Nature 2004; 432:466-472. doi: 10.1038/nature03000.
23. Philp D, Badamchian M, Scheremeta B, Nguyen M, Goldstein AL and Kleinman HK. Thymosin β4 and a synthetic peptide containing its actin-binding domain promote dermal wound repair in db/db diabetic mice and in aged mice. Wound Repair and Regeneration 2003; 11:19-24. doi:https://doi.org/10.1046/j.1524 475X.2003.11105.x.
24. Sosne G, Szliter EA, Barrett R, Kernacki KA, Kleinman H and Hazlett LD.Thymosin Beta 4 Promotes Corneal Wound Healing and Decreases Inflammation in Vivo Following Alkali Injury. *Exp Eye Res* 2002; 74:293-299. doi: https://doi.org/10.1006/exer.2001.1125.
25. Chatuphonprasert W and Jarukamjorn K. Effect of styrene oxide and diethyl maleate on expression of cytochrome P450 family 1 and glutathione store in mouse liver. *Trop J Pharm Res* 2021; 20:231-237.
26. Kilkenny C, Browne W, Cuthill IC, Emerson M and Altman DG. Animal research: reporting in vivo experiments: the ARRIVE guidelines. Br J Pharmacol 2010; 160:1577-9. doi: 10.1111/j.1476-5381.2010.00872.x.
27. Clark JD, Gebhart GF, Gonder JC, Keeling ME and Kohn DF. The 1996 Guide for the Care and Use of Laboratory Animals. ILAR Journal 1997; 38:41-48. doi: 10.1093/ilar.38.1.41
28. Suvarna KS, Layton C and Bancroft JD. Bancroft's theory and practice of histological techniques E-Book 2018; Elsevier health sciences.
29. Liu N, Guan Y, Zhou C, Wang Y, Ma Z and Yao S Pulmonary and Systemic Toxicity in a Rat Model of Pulmonary Alveolar Proteinosis Induced by Indium-Tin Oxide Nanoparticles. Int J Nanomedicine 2022; 17:713-731. doi: 10.2147/ijn.s338955.
30. Ellman GL. Tissue sulfhydryl groups. *Arch Biochem Biophys* 1959; 82:70-77. doi: https://doi.org/10.1016/0003-9861(59)90090-6.
31. Alsemeh AE and Abdullah DM. Protective effect of alogliptin against cyclophosphamide-induced lung toxicity in rats: Impact on PI3K/Akt/FoxO1 pathway and downstream inflammatory cascades. *Cell Tissue Res* 2022; 388:417-438. doi: 10.1007/s00441-022-03593-1.
32. Chitra P, Saiprasad G, Manikandan R and Sudhandiran G. Berberine attenuates bleomycin induced pulmonary toxicity and fibrosis via suppressing NF-κB dependant TGF-β1 activation: A biphasic experimental study. *Toxicol Lett* 2013; 219:178-193. doi: https://doi.org/10.1016/j.toxlet.2013.03.009

33. Zhang JM and An J. Cytokines, inflammation, and pain. Int Anesthesiol Clin 2007; 45:27-37. doi: 10.1097/AIA.0b013e318034194e
34. Padgett LE, Broniowska KA, Hansen PA, Corbett JA and Tse HM. The role of reactive oxygen species and proinflammatory cytokines in type 1 diabetes pathogenesis. *Ann N Y Acad Sci* 2013; 1281:16-35. doi: https://doi.org/10.1111/j.1749-6632.2012.06826.x.
35. Forrester SJ, Kikuchi DS, Hernandes MS, Xu Q and Griendling KK. Reactive Oxygen Species in Metabolic and Inflammatory Signaling. *Circ Res* 2018; 122:877-902. doi:10.1161/CIRCRESAHA.117.311401.
36. Kik K, Bukowska B and Sicińska P. Polystyrene nanoparticles: Sources, occurrence in the environment, distribution in tissues, accumulation and toxicity to various organisms. *Environ Pollut* 2020; 262:114297. doi: https://doi.org/10.1016/j.envpol.2020.114297.
37. Abozaid ER. Thymosin Beta 4 Improves the Intestinal Ischemia/Reperfusion Injury in Rats. *Am J Biomed Sci* 2020; 12.
38. Badamchian M, Fagarasan MO, Danner RL, Suffredini AF, Damavandy H and Goldstein AL . Thymosin β4 reduces lethality and down-regulates inflammatory mediators in endotoxin-induced septic shock. *Int Immunopharmacol* 2003; 3:1225-1233. doi: https://doi.org/10.1016/S1567-5769(03)00024-9.
39. Zheng XY, Lv YF, Li S, Li Q, Zhang QN, Zhang XT, et al. Recombinant adeno-associated virus carrying thymosin β(4) suppresses experimental colitis in mice. World J Gastroenterol 2017; 23:242-255. doi: 10.3748/wjg.v23.i2.242.
40. Daniil ZD, Papageorgiou E, Koutsokera A, Kostikas K, Kiropoulos T, Papaioannou AI, et al. Serum levels of oxidative stress as a marker of disease severity in idiopathic pulmonary fibrosis. Pulm Pharmacol Ther 2008; 21:26-31. doi: https://doi.org/10.1016/j.pupt.2006.10.005.
41. Fubini B and Hubbard A. Reactive oxygen species (ROS) and reactive nitrogen species (RNS) generation by silica in inflammation and fibrosis. *Free Radic Biol Med* 2003; 34:1507-1516. doi: https://doi.org/10.1016/S0891-5849(03)00149-7.
42. Bargagli E, Olivieri C, Bennett D, Prasse A, Muller-Quernheim J and Rottoli P. Oxidative stress in the pathogenesis of diffuse lung diseases: A review. *Respir Med* 2009; 103:1245-1256. doi: https://doi.org/10.1016/j.rmed.2009.04.014.
43. Haghighat M, Khavanin A and Allameh A. Oxidative stress indices in rats' lung tissues following simultaneous exposure to noise and styrene. *J Occup* Health 2017; 6:1-8. doi: 10.18869/acadpub.johe.6.1.1.
44. Wei C, Kumar S, Kim I-K and Gupta S. Thymosin beta 4 protects cardiomyocytes from oxidative stress by targeting anti-oxidative enzymes and anti-apoptotic genes. 2012; e42586.
45. Renga G, Oikonomou V, Moretti S, Stincardini C, Bellet MM, Pariano M, et al. Thymosin β4 promotes autophagy and repair via HIF-1α stabilization in chronic granulomatous disease. *Life Sci Alliance* 2019; 2:e201900432. doi: 10.26508/lsa.201900432.
46. Horowitz JC, Rogers DS, Sharma V, Vittal R, White ES, Cui Z, et al. Combinatorial activation of FAK and AKT by transforming growth factor-β1 confers an anoikis-resistant phenotype to myofibroblasts. *Cell Signal* 2007; 19:761-771. doi: https://doi.org/10.1016/j.cellsig.2006.10.001.
47. Tseng C-M, Hsiao Y-H, Su VY-F, Su K-C, Wu Y-C, Chang K-T, et al. The Suppression Effects of Thalidomide on Human Lung Fibroblasts: Cell Proliferation, Vascular Endothelial Growth Factor Release, and Collagen Production. Lung 2013; 191:361-368. doi: 10.1007/s00408-013-9477-1.
48. Kolodsick JE, Toews GB, Jakubzick C, Hogaboam C, Moore TA, McKenzie A, et al. Protection from fluorescein isothiocyanate-induced fibrosis in IL-13-deficient, but not IL-4-deficient, mice results from impaired collagen synthesis by fibroblasts. J Immunol 2004; 172:4068-76. doi: 10.4049/jimmunol.172.7.4068.
49. Wirsching H-G, Krishnan S, Florea A-M, Frei K, Krayenbühl N, Hasenbach K, et al. Thymosin beta 4 gene silencing decreases stemness and invasiveness in glioblastoma. Brain 2013; 137:433-448. doi: 10.1093/brain/awt333.
50. SMART N, RISEBRO CA, MELVILLE AAD, MOSES K, SCHWARTZ RJ, CHIEN KR, et al. Thymosin β-4 Is Essential for Coronary Vessel Development and Promotes Neovascularization via Adult Epicardium. *Ann N Y Acad Sci* 2007; 1112:171-188. doi: https://doi.org/10.1196/annals.1415.000.
51. Vancheri C, Sortino MA, Tomaselli V, Mastruzzo C, Condorelli F, Bellistrí G, et al. Different Expression of TNF-α Receptors and Prostaglandin E2Production in Normal and Fibrotic Lung Fibroblasts: Potential Implications for the Evolution of the Inflammatory Process. *Am J Respir Cell Mol Biol* 2000; 22:628-634.
52. Bozyk PD and Moore BB. Prostaglandin E2 and the pathogenesis of pulmonary fibrosis. *Am J Respir Cell Mol Biol* 2011; 45:445-452.
53. Maher TM, Evans IC, Bottoms SE, Mercer PF, Thorley AJ, Nicholson AG, et al. Diminished prostaglandin E2 contributes to the apoptosis paradox in idiopathic pulmonary fibrosis. Am J Respir Crit Care Med 2010; 182:73-82. doi: 10.1164/rccm.200905-0674OC.
54. Huang SK, Fisher AS, Scruggs AM, White ES, Hogaboam CM, Richardson BC, et al. Hypermethylation of PTGER2 Confers Prostaglandin E2 Resistance in Fibrotic Fibroblasts from Humans and Mice. Am J Pathol 2010; 177:2245-2255. doi: https://doi.org/10.2353/ajpath.2010.100446.
55. Hwang D, Kang MJ, Jo MJ, Seo YB, Park NG and Kim GD. Anti-inflammatory activity of β-thymosin peptide derived from pacific oyster (Crassostrea gigas) on NO and PGE2 production by down-

regulating NF-κB in LPS-induced RAW264. 7 macrophage cells. Marine drugs 2019; 17(2), 129. doi: 10.3390/md17020129
56. Csanády GA, Kessler W, Hoffmann HD and Filser JG. A toxicokinetic model for styrene and its metabolite styrene-7,8-oxide in mouse, rat and human with special emphasis on the lung. *Toxicol Lett* 2003; 138:75-102. doi: https://doi.org/10.1016/S0378-4274(02)00409-5.
57. Haghighat M, Allameh A, Fereidan M, Khavanin A and Ghasemi Z. Effects of concomitant exposure to styrene and intense noise on rats' whole lung tissues. Biochemical and histopathological studies. Drug Chem Toxicol 2022; 45:120-126. doi: 10.1080/01480545.2019.1662033.
58. Kaufmann W, Mellert W, van Ravenzwaay B, Landsiedel R and Poole A. Effects of styrene and its metabolites on different lung compartments of the mouse—cell proliferation and histomorphology. Regul Toxicol Pharmacol 2005; 42:24-36. doi: https://doi.org/10.1016/j.yrtph.2005.01.002.
59. Yaman OM, Guner I, Guntas G, Sonmez OF, Tanriverdi G, Cakiris A, et al. Protective Effect of Thymosin β4 against Abdominal Aortic Ischemia–Reperfusion-Induced Acute Lung Injury in Rats. Medicina 2019; 55:187.
60. Gilbane AJ, Denton CP and Holmes AM. Scleroderma pathogenesis: a pivotal role for fibroblasts as effector cells. Arthritis Res Ther 2013; 15:215. doi: 10.1186/ar4230
61. Kendall RT and Feghali-Bostwick CA. Fibroblasts in fibrosis: novel roles and mediators. Front Pharmacol 2014; doi: 10.3389/fphar.2014.00123.
62. Rubio L, Marcos R and Hernández A. Potential adverse health effects of ingested micro- and nanoplastics on humans. Lessons learned from in vivo and in vitro mammalian models. J Toxicol Environ, Part B 2020; 23:51-68. doi: 10.1080/10937404.2019.1700598.
63. Galloway TS. Micro-and nano-plastics and human health. Marine anthropogenic litter, Springer, Cham 2015; 343-366.
64. Zhang X, Huang H, Chang H and Jin X. Magnolol reduces bleomycin-induced rodent lung fibrosis. Int J Clin Exp Med 2015; 8:15450-7.
65. Dijkstra CD, Döpp EA, Joling P and Kraal G. The Heterogeneity of Mononuclear Phagocytes in Lymphoid Organs: Distinct Macrophage Subpopulations in Rat Recognized by Monoclonal Antibodies ED1, ED2 and ED3. In: Klaus GGB (ed) Microenvironments in the Lymphoid System, Springer US 1985; Boston, MA pp. 409-419.
66. Daghigh F, Alihemmati A, Karimi P, Habibi P and Ahmadiasl N. Genistein preserves the lungs of ovariectomized diabetic rats: addition to apoptotic and inflammatory markers in the lung. Iran J Basic Med Sci 2017; 20:1312-1317. doi: 10.22038/ijbms.2017.9599
67. Fehrenbach H, Kasper M, Haase M, Schuh D and Müller M. Differential immunolocalization of VEGF in rat and human adult lung, and in experimental rat lung fibrosis: Light, fluorescence, and electron microscopy. Anat Rec 1999; 254:61-73. doi: https://doi.org/10.1002/(SICI)1097-0185(19990101)254:1<61::AID-AR8>3.0.CO;2-D.
68. Gao L, Jiang D, Geng J, Dong R and Dai H. Hydrogen inhalation attenuated bleomycin-induced pulmonary fibrosis by inhibiting transforming growth factor-β1 and relevant oxidative stress and epithelial-to-mesenchymal transition. Exp Physiol 2019; 104:1942-1951. doi: https://doi.org/10.1113/EP088028.
69. Hamada N, Kuwano K, Yamada M, Hagimoto N, Hiasa K, Egashira K, et al. Anti-Vascular Endothelial Growth Factor Gene Therapy Attenuates Lung Injury and Fibrosis in Mice1. J Immunol. 2005; 175:1224-1231. doi: 10.4049/jimmunol.175.2.1224.
70. Kleinman HK, Kulik V and Goldstein AL. Prepared for special issue on thymosins Thymosin β4 and the anti-fibrotic switch. Int Immunopharmacol. 2023; 115:109628. doi: https://doi.org/10.1016/j.intimp.2022.109628.

To Cite:

Abdelwahab, O., Abozaid, E., Abdel-Kareem, R. Pneumotoxicity of Styrene Oxide and the Possible Protective Role of Thymosin β4 in Albino Rat: Biochemical and Immunohistochemical Study. *Zagazig University Medical Journal*, 2023; (728-745): -. doi: 10.21608/zumj.2023.190394.2737